
VISIONCOACH: Reinforcing Grounded Video Reasoning via Visual-Perception Prompting

Daeun Lee Shoubin Yu Yue Zhang Mohit Bansal

University of North Carolina, Chapel Hill
{daeun, shoubin, yuezhan, mbansal}@cs.unc.edu

 Code  Project page  Model

Abstract

Video reasoning requires models to locate and track question-relevant evidence across frames. While reinforcement learning (RL) with verifiable rewards improves accuracy, it still struggles to achieve reliable spatio-temporal grounding during the reasoning process. Moreover, improving grounding typically relies on scaled training data or inference-time perception tools, which increases annotation cost or computational cost. To address this challenge, we propose VISIONCOACH, an input-adaptive RL framework that improves spatio-temporal grounding through visual prompting as training-time guidance. During RL training, visual prompts are selectively applied to challenging inputs to amplify question-relevant evidence and suppress distractors. The model then internalizes these improvements through self-distillation, enabling grounded reasoning directly on raw videos without visual prompting at inference. VISIONCOACH consists of two components: (1) Visual Prompt Selector, which predicts appropriate prompt types conditioned on the video and question, and (2) Spatio-Temporal Reasoner, optimized with RL under visual prompt guidance and object-aware grounding rewards that enforce object identity consistency and multi-region bounding-box overlap. Extensive experiments demonstrate that VISIONCOACH achieves state-of-the-art performance under comparable settings, across diverse video reasoning, video understanding, and temporal grounding benchmarks (V-STAR, VideoMME, World-Sense, VideoMMU, PerceptionTest, and Charades-STA), while maintaining a single efficient inference pathway without external tools. Our results show that visual prompting during training improves grounded video reasoning, while self-distillation enables the model to internalize this ability without requiring prompts at inference time.

1 Introduction

Recent advances in reinforcement learning (RL) with verifiable rewards [Liu et al., 2024a] have begun to improve multimodal reasoning and are increasingly applied to video reasoning [Cheng et al., 2025a, Fu et al., 2025, Hu et al., 2025, Deng et al., 2025b]. Despite recent progress, existing video reasoning approaches still struggle to achieve reliable spatio-temporal grounding throughout the reasoning process. Text-centric video reasoning models [Feng et al., 2025, Wang et al., 2025b, Lee et al., 2025] (Figure 1 (a)) often generate hallucinated explanations driven by language priors rather than faithful visual observations. Visual tool-calling approaches [Yan et al., 2025, Rasheed et al., 2025, Ge et al., 2025, Zhang et al., 2025b, Meng et al., 2025, Zeng et al., 2026] (Figure 1 (b)) improve grounding by invoking external perception tools such as temporal clipping or zoom-in. While these tools can retrieve relevant evidence, they introduce additional computational overhead due to repeated tool invocation and multi-stage processing during inference. Recent grounded reasoning models [Meng et al., 2025] (Figure 1 (c)) attempt to integrate spatio-temporal evidence within a

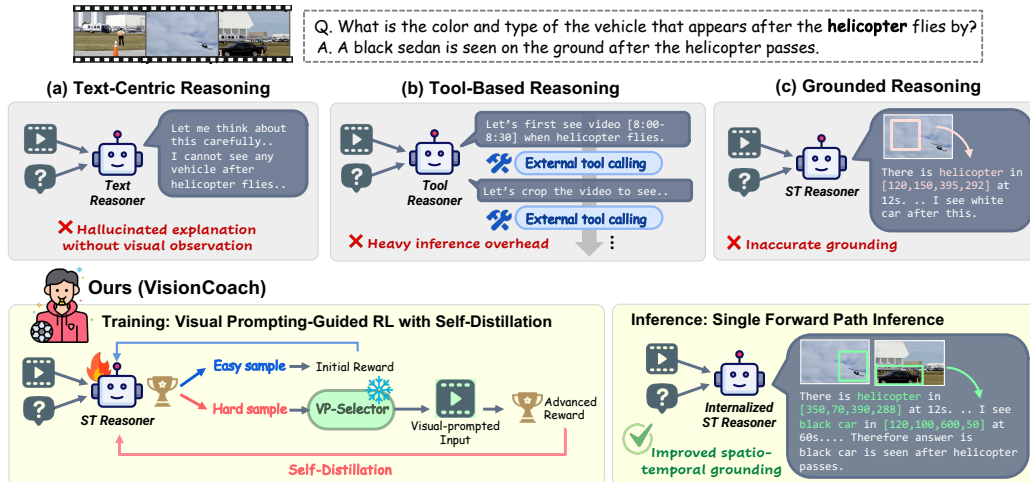


Figure 1: **Comparison with previous video reasoning methods and VISIONCOACH.** VISIONCOACH leverages visual-prompt guided RL with self-distillation to internalize improved spatio-temporal grounding behaviors induced by visual guidance. During inference, it maintains a single forward-pass reasoning while achieving enhanced grounding performance.

single model by interleaving grounding and reasoning. Nevertheless, grounding remains unreliable, frequently producing inaccurate object references or hallucinated bounding boxes that propagate errors during reasoning.

At the core of this issue is the absence of mechanisms that enforce alignment between intermediate reasoning steps and spatio-temporal evidence. In practice, improving grounding typically requires either scaling training data Meng et al. [2025], Yan et al. [2025], Li et al. [2025] or additional perception modules Tian et al. [2025], Yang et al. [2025] (e.g., cropping image regions or trimming the video) at inference time. However, dense annotations across diverse video datasets are expensive to obtain, while inference-time tools increase computational overhead. These solutions improve grounding only through heavier external intervention, rather than enhancing the model’s intrinsic perception behavior. Instead, we shift the focus from data scaling and inference-time intervention to **training-time guidance**, aiming to internalize grounded reasoning behavior while preserving a lightweight inference pipeline.

To this end, we propose VISIONCOACH, an input-adaptive RL framework that uses visual prompts as a training-time vision coach to improve spatio-temporal grounding while enabling inference directly on raw videos. The key idea is to selectively apply visual prompts to challenging inputs during RL training to strengthen grounding, and to internalize these improvements through self-distillation so that visual prompting is no longer required at inference. Instead of relying solely on implicit feature-space attention, VISIONCOACH performs reasoning-driven perception control at the input level, amplifying question-relevant evidence and suppressing distractors during training.

As illustrated in Figure 2, VISIONCOACH consists of two key components: a Visual Prompt Selector (VP-SELECTOR) and a Spatio-Temporal Reasoner (ST-REASONER). VP-SELECTOR predicts an appropriate visual prompt type conditioned on the video and question to provide adaptive perception guidance for challenging inputs. To train VP-SELECTOR, we first construct a visual prompting candidate dataset using a proxy reasoner. Based on this dataset, VP-SELECTOR is optimized with SFT to select the most effective visual prompt type. ST-REASONER performs grounded reasoning under visual prompt-guided perception and is optimized with RL using grounding-aware rewards. During the ST-REASONER training, hard samples are identified based on initial rewards, and the frozen VP-SELECTOR predicts visual prompt types that guide the ST-REASONER to attend to relevant regions and moments, producing more grounded reasoning trajectories. To further strengthen grounded reasoning, we introduce an *object-aware spatial grounding reward* that enforces object identity consistency and average IoU across multiple predicted bounding boxes, encouraging accurate multi-object grounding and temporally consistent reasoning. To remove prompt dependency at inference time, we employ *self-distillation*, where the prompted input serves as a coach to guide the

policy model, enabling grounded perception behavior to be internalized. At inference, the model performs reasoning directly on raw videos with a *single* forward pass, without visual prompting. Together, these designs provide localized perception guidance during training while maintaining a simple and efficient inference pipeline.

We evaluate VISIONCOACH on the (1) spatio-temporal reasoning benchmark V-STAR [Cheng et al., 2025b], (2) general video understanding benchmarks (VideoMME [Fu et al., 2025], WorldSense [Hong et al., 2025a], VideoMMU [Hu et al., 2025], and PerceptionTest [Patraucean et al., 2023]), and (3) temporal grounding benchmark (Charades-STA [Gao et al., 2017]). On V-STAR, VISIONCOACH surpasses GPT-4o and improves over Qwen2.5-VL-7B by +15.0% mAM and +25.1% mLGM, establishing new state-of-the-art performance. In general video understanding and temporal grounding benchmarks, it consistently outperforms prior open-source VideoLLMs, demonstrating strong performance in long-video reasoning and perception-oriented understanding tasks. We further provide comprehensive analyses, including spatio-temporal attention map visualization, component-wise ablation, generalization effect of VP-SELECTOR across different backbone models, and statistics of adaptive visual prompting.

Our contributions are summarized as follows:

- We propose an input-adaptive RL framework for video reasoning that explicitly guides spatio-temporal grounding through training-time visual prompting and self-distillation, enabling the reasoning model to internalize grounded perception without requiring visual prompts at inference.
- We design an object-aware spatial grounding reward that incorporates object identity consistency and multi-region bounding-box IoU to better support spatial-grounded reasoning.
- We introduce a visual prompt selector with a proxy-reasoner-based data construction pipeline to predict appropriate visual prompts for video QA inputs.
- Extensive experiments and analyses demonstrate that VISIONCOACH achieves SoTA performance across a wide range of video reasoning, video understanding, and temporal grounding benchmarks.

2 Related Work

Video Reasoning. Video understanding has advanced rapidly with large multimodal models [Li et al., 2024a, Bai et al., 2025a, Li et al., 2023], enabling complex video QA and reasoning across diverse areas [Fu et al., 2025, Hu et al., 2025, Patraucean et al., 2023, Cheng et al., 2025b, Hong et al., 2025b, Deng et al., 2025c, Wu et al., 2024a, Deng et al., 2025a, Yu et al., 2026]. Despite progress, reliable *grounded* video reasoning remains challenging because models must track object states, events, and interactions over time. A growing line of work applies reinforcement learning with verifiable or rule-based rewards to strengthen multimodal reasoning [Guo et al., 2025, Li et al., 2025, Yan et al., 2025, Zhang et al., 2025b, Meng et al., 2025, Zeng et al., 2026, Wang et al., 2025d, Chen et al., 2025b, Cheng et al., 2026], but existing approaches often either (i) remain text-centric and hallucinate evidence, or (ii) rely on iterative tool operations at inference time (e.g., progressive ROI localization), introducing overhead and leaving limited explicit control over dense spatio-temporal evidence. Our work targets this gap by using *training-time* perception control to improve grounding.

Visual Prompting. Visual prompting [Wu et al., 2024b] augments inputs with lightweight visual cues (e.g., boxes, masks, points, scribbles, overlays) to steer attention and improve localized understanding without heavy architectural changes. Early and concurrent studies show that simple edits in pixel space, such as drawing a red circle around an object, can reliably direct VLM attention [Shtedritski et al., 2023]. Recent work expands visual prompting to general vision understanding in MLLMs [Cai et al., 2024, Li et al., 2024b, Choudhury et al., 2024, Gu et al., 2025]. For video settings, prompting has also been used to improve temporal grounding by adding structured cues such as per-frame numbering [Wu et al., 2024c, Zhang et al., 2025c]. Meanwhile, learned or automated prompting methods aim to *select* or *retrieve* effective prompts conditioned on the input, improving robustness and usability [Zhang et al., 2025d, 2024a]. In VISIONCOACH, we use adaptive prompting *only during RL training* and then internalize the benefit so inference no longer depends on prompting.

Model Distillation. Knowledge distillation transfers behavior from a stronger teacher to a student model, improving efficiency and robustness [Hinton et al., 2015]. Beyond classical teacher-student training, self-distillation and iterative teacher replacement can further improve generalization without additional labels [Furlanello et al., 2018]. Distillation has also been used in sequential decision

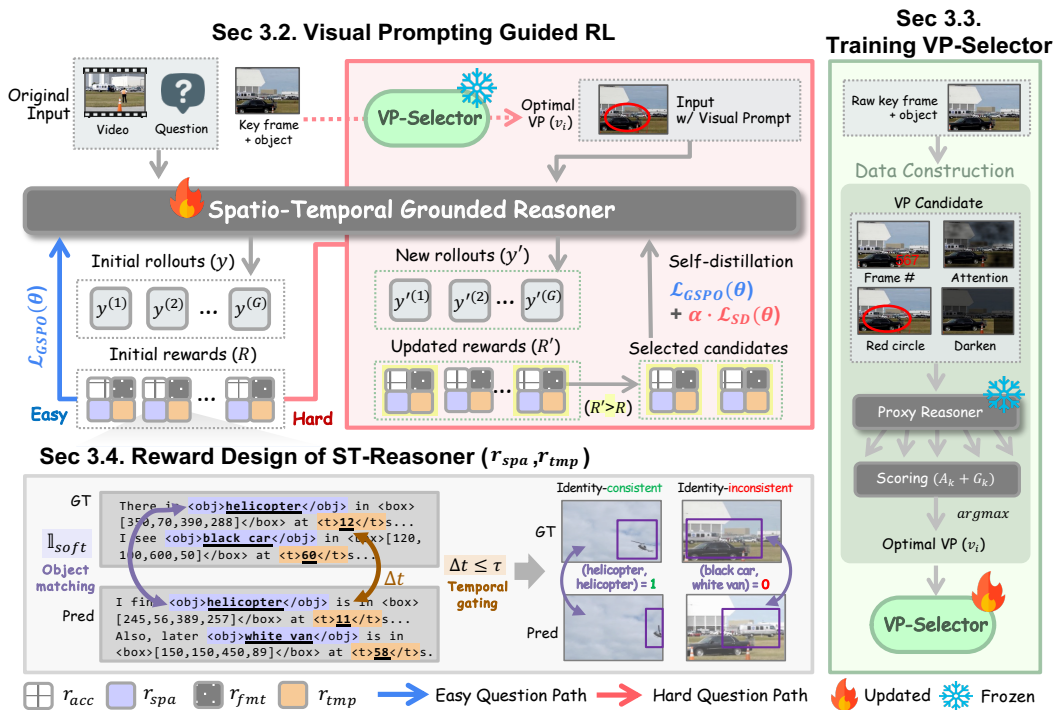


Figure 2: **Detailed Architecture of VISIONCOACH.** We introduce VISIONCOACH, a visual-prompt-guided RL framework for training a spatio-temporally grounded reasoner (Section 3.2). The framework includes Visual Prompt Selector (VP-SELECTOR) that predicts optimal visual prompts (Section 3.3), and object-aware spatial grounding rewards that enforce object identity consistency and multiple predicted bounding boxes (Section 3.4).

making (policy distillation) to compress or unify behaviors learned via RL [Rusu et al., 2015]. In VISIONCOACH, self-distillation helps the ST-Reasoner *internalize* the grounding improvements induced by visual prompting guided training trajectories, enabling a single, prompt-free inference.

3 Method

As shown in Figure 2, we propose VISIONCOACH, an input-adaptive RL framework that improves spatio-temporal grounding in video reasoning through visual prompting guidance. We begin by formalizing spatio-temporal grounded reasoning and presenting the motivation for our approach (Section 3.1). Next, we introduce the overall training pipeline of VISIONCOACH in Section 3.2, which integrates visual prompting with RL and self-distillation to encourage grounded reasoning. Finally, we describe the key components in detail: the Visual Prompt Selector (Section 3.3), which predicts input-adaptive visual prompts, followed by the reward design of Spatio-Temporal Reasoner (Section 3.4), which learns grounded reasoning from prompt-guided training signals and grounding-aware rewards.

3.1 Problem Statement and Motivation

Given an input video x and a question q , the goal of video QA is to generate a grounded reasoning trajectory y and predict the final answer a over complex and dynamic visual content. Unlike text-based reasoning (Figure 1 (a)), our reasoning requires a policy model π_θ to integrate explicit spatio-temporal grounding, identifying when and where relevant evidence occurs while reasoning.

Motivation. To better understand the relationship between grounding and answering performance, we analyze model behaviors on the PerceptionTest Patraucean et al. [2023] subset. As shown in Figure 3, correctly answered samples consistently exhibit higher temporal alignment, object identity matching, and spatial IoU compared to incorrectly answered ones, indicating that accurate spatio-temporal grounding is correlated with correct answering. We further investigate how different visual prompts affect answering performance.

As shown in Table 1, different prompts lead to different results, suggesting that selecting an appropriate visual prompt is crucial for effective answering Wu et al. [2024c], Zhang et al. [2025d,c]. Notably, the oracle prompt selection achieves significantly higher accuracy, indicating that adaptive perceptual guidance can substantially improve downstream answering when the appropriate prompt is applied. Motivated by these empirical observations, we propose an RL framework that enables input-adaptive visual prompting, allowing the model to dynamically select suitable prompts based on the input context, thereby achieving more reliable grounding and question answering.

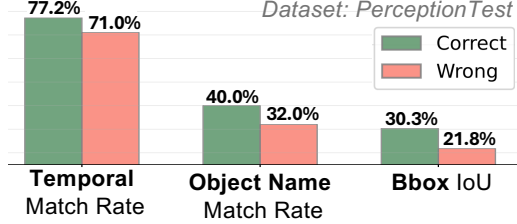


Figure 3: Grounding effect on answering.

Models	Raw key frame	Darken	Red circle	Oracle (Any-corr)
Qwen2.5-VL	52.2	43.3	51.5	70.8
Gemini-2.5-Flash	47.4	50.4	49.3	75.2

Table 1: Effect of different visual prompting types.

3.2 VISIONCOACH: VP-Guided RL with Self-Distillation

We introduce VISIONCOACH, an RL framework that integrates VP-SELECTOR and ST-REASONER to enable input-adaptive visual guidance during training. We describe each component in detail in Section 3.3 (VP-SELECTOR) and Section 3.4 (Reward design for ST-REASONER). The ST-REASONER π_θ is optimized using GSPO Zheng et al. [2025], starting from a cold-start initialization and trained on video-question pairs (x, q) . For each input, G reasoning trajectories are sampled and evaluated with grounding-aware rewards. Visual prompts are selectively applied to challenging inputs during RL to strengthen spatio-temporal grounding, and their benefits are internalized through self-distillation, eliminating the need for visual prompting at inference. The overall training procedure is shown in Algorithm 1 and top left in Figure 2.

Input-adaptive hard sample identification. Given an input (x_i, q_i) , we first perform G initial rollouts using the current policy. Let $\{R_i^{(g)}\}_{g=1}^G$ denote the resulting overall rewards. We compute the average reward \bar{R}_i and classify the sample as hard if $\bar{R}_i < k$, where k is a predefined threshold for hard sample filtering. This input-adaptive mechanism determines whether additional visual guidance is necessary for each example, allowing more targeted visual prompting to help with grounding.

Visual prompting guidance generation. For hard samples, we feed (x_i, q_i) into the trained VP-SELECTOR, which is elaborated in later Section 3.3 to obtain the optimal visual prompt (such as darken, which is denoted as) v_i . We then apply this prompt to the key frames of x_i to construct a visual-prompted input x'_i , and append a textual hint describing the applied visual prompting to the original question q_i and make q'_i . The visual prompt introduces localized cues that facilitate spatio-temporal grounding. For example, suppressing irrelevant regions can emphasize key object areas and improve spatial reasoning. Using the prompted input (x'_i, q'_i) , we perform another G rollouts and obtain new reasoning y'_i and updated overall rewards $\{R_i'^{(g)}\}_{g=1}^G$. We expect improved reasoning trajectories and higher rewards due to the enhanced grounding provided by visual prompting. Detailed ablation studies on the choice of reward for candidate selection are in Appendix D.

Self-distillation. When visual prompting yields improved rewards, we further reinforce these improved reasoning through self-distillation. Specifically, after performing rollouts on the visual-prompted input, we identify the subset of rollouts whose overall rewards exceed the average reward of the original rollouts, i.e., $C_i = \{g \mid R_i'^{(g)} > \bar{R}_i\}$. Among these candidates, we select the top N rollouts S_i based on answering rewards. If no such candidates exist (i.e., $C_i = \emptyset$), we skip the self-distillation step for the current sample. We then apply token-level negative log-likelihood (NLL) to the selected reasoning:

$$\mathcal{L}_{SD}(\theta) = -\frac{1}{|S_i|} \sum_{j \in S_i} \frac{1}{|y'_{i,j}|} \sum_{t=1}^{|y'_{i,j}|} \log \pi_\theta(y'_{i,j,t} \mid y'_{i,j,<t}, x'_i, q'_i). \quad (1)$$

This objective encourages the policy to internalize high-reward reasoning trajectories generated under visual guidance. Accordingly, the final training objective is defined as:

$$\mathcal{L}_{GSPO}(\theta) + \alpha \mathbb{I}_i \mathcal{L}_{SD}(\theta), \quad (2)$$

Algorithm 1 VISIONCOACH: Visual Prompt Guided RL with Self-Distillation

Require: Dataset $\mathcal{D} = \{(x_i, q_i)\}_{i=1}^N$, ST-REASONER π_θ , trained VP-SELECTOR, reward r , number of rollouts G , hard question threshold k , self-distillation weight α .

```
1: for each  $(x_i, q_i) \in \mathcal{D}$  do
2:   for  $g \leftarrow 1$  to  $G$  do
3:      $y_i^{(g)} \sim \pi_\theta(\cdot | x_i, q_i)$ ,  $R_i^{(g)} \leftarrow r(x_i, y_i^{(g)})$            /* Conduct initial rollout
4:   end for
5:    $\bar{R}_i \leftarrow \frac{1}{G} \sum_{g=1}^G R_i^{(g)}$ ,  $\mathbb{I}_i \leftarrow \mathbf{1}[\bar{R}_i < k]$ 
6:   if  $\mathbb{I}_i = 1$  then                                           /* Generate VP guidance
7:      $v_i \leftarrow \text{VP-SELECTOR}(x_i, q_i)$ 
8:      $(x'_i, q'_i) \leftarrow (\text{VP}(x_i; v_i), q_i \oplus \text{hint}(v_i))$ 
9:     for  $g \leftarrow 1$  to  $G$  do
10:       $y_i'^{(g)} \sim \pi_\theta(\cdot | x'_i, q'_i)$ ,  $R_i'^{(g)} \leftarrow r(x'_i, y_i'^{(g)})$ 
11:    end for
12:     $\bar{R}'_i \leftarrow \frac{1}{G} \sum_{g=1}^G R_i'^{(g)}$ ,  $C_i \leftarrow \{g : R_i'^{(g)} > \bar{R}_i\}$ 
13:    if  $C_i \neq \emptyset$  then                                       /* Conduct self-distillation
14:       $S_i \leftarrow \text{TopN}(\{R_{i,\text{ans}}'^{(g)}\}_{g \in C_i})$ 
15:       $\mathcal{L}_{\text{SD}}(\theta) \leftarrow -\frac{1}{|S_i|} \sum_{j \in S_i} \frac{1}{|y_{i,j}'|} \sum_{t=1}^{|y_{i,j}'|} \log \pi_\theta(y_{i,j,t}' | y_{i,j,<t}') x'_i, q'_i$ 
16:       $\mathcal{L}(\theta) \leftarrow \mathcal{L}_{\text{GSPO}}(\theta) + \alpha \cdot \mathbb{I}_i \cdot \mathcal{L}_{\text{SD}}(\theta)$ 
17:    end if
18:  else
19:     $\mathcal{L}(\theta) \leftarrow \mathcal{L}_{\text{GSPO}}(\theta)$ 
20:  end if
21: end for
```

where \mathbb{I}_i is an indicator function that equals 1 if sample i is identified as a hard sample, and 0 otherwise. By repeatedly reinforcing improved trajectories, the model progressively internalizes the grounding behaviors induced by visual prompting, enabling self-evolving and more robust spatio-temporal reasoning without requiring visual prompts at inference time.

3.3 VP-SELECTOR: Learning to Provide Visual Guidance

We now introduce VP-SELECTOR, which is used to train the policy model ST-REASONER within our input-adaptive RL framework. Our VP-SELECTOR is designed to predict an input-adaptive visual prompt conditioned on the video-question pair, enabling targeted visual guidance during RL training for hard examples. Given an input (x, q) , the VP-SELECTOR selects an appropriate visual prompt v_i from a candidate pool, where each prompt provides a different form of perceptual guidance. As shown in Figure 2 right, we first construct a training dataset using proxy reasoners Google DeepMind [2025], Hurst et al. [2024], Bai et al. [2025a] to estimate the effectiveness of candidate prompts and train the small VLM to predict the most suitable visual prompt.

Training data collection. Since defining a gold visual prompt across models is challenging, we collect (x, v_i) pairs using multiple proxy reasoners to capture general prompt effectiveness patterns. We first define a visual prompt candidate $\mathcal{V} = \{v_1, v_2, \dots\}$ by applying diverse visual prompting to key frames and objects from x . Specifically, we consider red circles Shtedritski et al. [2023], attention-based prompts Yu et al. [2024], frame numbering Wu et al. [2024c], and darkening as potential visual guidance. For each candidate prompt v_k , we generate a visual-prompted input $x'_k = \text{VP}(x; v_k)$ and obtain reasoning outputs $y_k = \mathcal{R}(x'_k, q)$ using multiple proxy reasoners \mathcal{R} Comanici et al. [2025], Hurst et al. [2024], Bai et al. [2025a]. We compute binary answer accuracy and grounding scores (A_k, G_k) , average them across proxy reasoners, and select the optimal prompt as

$$v_i = \arg \max_{v_k \in \mathcal{V}} (A_k + G_k). \quad (3)$$

The resulting (x, q, v_i) pairs are used to train the VP-Selector to predict the optimal prompt conditioned on the input video and question. Please check Appendix C.2 for more data details.

Training. Given the collected dataset $\mathcal{D} = \{(x, q, v_i)\}$, we train the VP-SELECTOR as a lightweight VLM classifier Bai et al. [2025b] with LoRA Hu et al. [2022]. We cast prompt selection as a $|\mathcal{V}|$ -way prediction problem and optimize the selector using a supervised objective. Concretely, we format the input (x, q) as an instruction to choose one method from \mathcal{V} and train the model to generate the corresponding prompt label as a single-token/short-string response using token-level cross-entropy loss. The VP-SELECTOR is frozen when incorporated in the RL framework. Additional details are provided in Appendix C.4.

3.4 Reward Design of ST-REASONER

We design reward functions to train ST-REASONER with GSPO. Specifically, we employ four reward components: (1) answer accuracy, (2) format correctness, (3) temporal grounding, and (4) object-aware spatial grounding. Among them, the object-aware spatial grounding reward is newly introduced in this work, while the remaining rewards follow prior work Meng et al. [2025]. The overall reward:

$$r(x, y) = r_{\text{acc}}(x, y) + r_{\text{fmt}}(x, y) + r_{\text{tmp}}(x, y) + r_{\text{spa}}(x, y), \quad (4)$$

and the rewards are group-normalized across rollouts to compute advantages used for GSPO updates.

Accuracy reward (r_{acc}). Following Meng et al. [2025], we define task-specific accuracy rewards depending on the supervision type. For multiple-choice questions, the reward is binary correctness. For open-ended questions, we compute textual similarity between the predicted and ground-truth answers using ROUGE. For spatial grounding tasks, the reward is given by the visual IoU between predicted and GT bounding boxes, while for temporal grounding tasks we use temporal IoU between predicted and GT time intervals. This design provides a unified accuracy signal that adapts to heterogeneous task formats.

Format reward (r_{fmt}). We assign a binary reward that evaluates whether the generated output follows the required structured format, including the correct use of `<think>` and `<answer>` tags as well as valid `<obj>`, `<box>`, and `<t>` annotations. Outputs that satisfy the format receive a reward of 1, and 0 otherwise.

Temporal grounding reward (r_{tmp}). Following prior work Meng et al. [2025], we set the temporal grounding reward to force the model locate correct temporal boundaries for visual evidence. Let $\mathcal{T}^{\text{gt}} \subset \mathbb{R}$ denote the set of annotated ground-truth temporal positions. Depending on the training dataset, annotations are provided either as discrete timestamps or as temporal intervals. When interval annotations are available, we denote the ground-truth interval set as $\mathcal{S}^{\text{gt}} = \{[s_\ell^{\text{gt}}, e_\ell^{\text{gt}}]\}_{\ell=1}^L$. From the generated reasoning y , we parse M predicted timestamps $\{t_m\}_{m=1}^M$. For each t_m , we first match it to the closest ground-truth temporal position:

$$\tilde{t}_m = \arg \min_{t \in \mathcal{T}^{\text{gt}}} |t_m - t|, \quad \Delta t_m = |t_m - \tilde{t}_m|.$$

Then, we define the temporal reward as

$$r_{\text{tmp}}(x, y) = \frac{1}{M} \sum_{m=1}^M r_m, \quad (5)$$

where

$$r_m = \begin{cases} 1, & \text{if } \exists \ell : t_m \in [s_\ell^{\text{gt}}, e_\ell^{\text{gt}}], \\ \exp\left(-\frac{\Delta t_m^2}{2\sigma^2}\right), & \text{otherwise.} \end{cases} \quad (6)$$

Object-aware spatial grounding reward (r_{spa}). Here, we further design object-aware spatial grounding reward to better support grounded reasoning. Prior work Meng et al. [2025] computes spatial rewards by selecting only the predicted bounding box with the maximum IoU, without considering object identity. However, we observe that this design encourages single-box predictions and object-agnostic hallucinations, as it does not enforce consistency between the predicted objects and the grounded region. As shown in the bottom of Figure 2, to promote accurate object identification and multi-object grounding, we introduce a spatial reward that jointly considers soft object identity matching and all predicted box IoUs under temporal gating.

From the generated reasoning y , we parse predicted objects and bounding boxes to construct spatio-temporal tuples $\{(o_m, t_m, b_m)\}_{m=1}^M$, where o_m denotes the predicted object name and b_m denotes

Table 2: **Performance on the V-STAR benchmark.** VISIONCOACH achieve strong spatio-temporal reasoning across overall dimensions.

Model	What	When (Temporal IoU)		Where (Spatial IoU)		Overall	
	Acc	Chain1	Chain2	Chain1	Chain2	mAM	mLGM
<i>Proprietary Models</i>							
Gemini-2-Flash Google DeepMind [2025]	53.0	24.5	23.8	4.6	2.2	26.9	35.6
GPT-4o Hurst et al. [2024]	60.8	16.7	12.8	6.5	3.0	26.8	38.2
<i>Open-source Models</i>							
TRACE Guo et al. [2024]	17.6	19.1	17.1	0.0	0.0	12.0	13.3
Oryx-1.5-7B Liu et al. [2024b]	20.5	13.5	14.8	10.1	3.5	15.1	13.8
VideoChat2 Li et al. [2024c]	36.2	13.7	12.5	2.5	1.0	17.0	20.3
Qwen2.5-VL-7B* Bai et al. [2025b]	33.5	15.4	13.8	17.0	2.5	19.3	22.4
InternVL-2.5-8B Chen et al. [2024]	44.2	8.7	7.8	0.7	0.1	17.6	24.9
Video-LLaMA3 Zhang et al. [2025a]	41.9	23.0	23.1	0.9	0.2	21.7	27.0
LLaVA-Video Zhang et al. [2024b]	49.5	10.5	12.2	1.9	1.3	20.8	27.3
Open-o3-video* Meng et al. [2025]	60.2	25.0	24.5	24.8	5.9	33.4	46.0
VISIONCOACH (Ours)	61.1	25.7	25.4	27.2	5.3	34.3	47.5
Δ vs. Qwen2.5-VL-7B	+27.6	+10.3	+11.6	+10.2	+2.8	+15.0	+25.1

the predicted bounding box. We denote the ground-truth object set and their bounding boxes at the matched keyframe \tilde{t}_m as $\mathcal{O}^{\text{gt}}(\tilde{t}_m)$ and $\mathcal{B}^{\text{gt}}(\tilde{t}_m)$, respectively. Using soft identity matching $\mathbb{I}_{\text{soft}}(o_m, o)$, we define the identity-consistent object set as

$$\mathcal{O}_m^{\text{match}} = \{o \in \mathcal{O}^{\text{gt}}(\tilde{t}_m) \mid \mathbb{I}_{\text{soft}}(o_m, o) = 1\}. \quad (7)$$

Here $\mathbb{I}_{\text{soft}}(o_m, o) = 1$ if the predicted object name o_m and the ground-truth name o satisfy one of the following conditions: (i) exact string match, (ii) substring inclusion (i.e., $o_m \subset o$ or $o \subset o_m$); otherwise $\mathbb{I}_{\text{soft}}(o_m, o) = 0$.

Moreover, since spatial grounding is meaningful only when temporal localization is sufficiently accurate, we apply **temporal gating** based on the deviation Δt_m defined above. We retain only predictions that satisfy temporal alignment and identity consistency:

$$\mathcal{I} = \{m \mid \Delta t_m \leq \tau \wedge |\mathcal{O}_m^{\text{match}}| > 0\},$$

where τ is a predefined temporal tolerance threshold. The spatial reward is then computed by averaging IoU scores over all valid predictions:

$$r_{\text{spa}}(x, y) = \frac{1}{|\mathcal{I}|} \sum_{m \in \mathcal{I}} \frac{1}{|\mathcal{O}_m^{\text{match}}|} \sum_{o \in \mathcal{O}_m^{\text{match}}} \max_{b^{\text{gt}} \in \mathcal{B}^{\text{gt}}(\tilde{t}_m)} \text{IoU}(b_m, b^{\text{gt}}). \quad (8)$$

4 Experiments

4.1 Setup

Implementation Details. For ST-REASONER training, we follow a two-stage pipeline consisting of SFT-based cold-start initialization followed by RL, consistent with prior work Meng et al. [2025], Feng et al. [2025], Wang et al. [2025b]. We first train the VP-SELECTOR and keep it frozen during the subsequent ST-REASONER training stage. The VP-SELECTOR is trained using the training dataset of TVQA+ Lei et al. [2020] and VideoEspresso Han et al. [2025]. For ST-REASONER training, we adopt the same SFT and RL datasets as Meng et al. [2025] to ensure a fair comparison. For self-distillation, we select the top-2 samples among candidates with improved rewards and set the self-distillation weight to $\alpha = 0.1$. Additional implementation details, baseline details, and threshold ablations are provided in Appendices B and D.

Benchmark and Metrics. We evaluate spatio-temporal reasoning on V-STAR Cheng et al. [2025b]. For zero-shot general video understanding, we report results on WorldSense Hong et al. [2025b], VideoMMU Hu et al. [2025], PerceptionTest Patraucean et al. [2023], and VideoMME Fu et al. [2025]. For zero-shot temporal grounding, we use Charades-STA Gao et al. [2017]. More details regarding metrics and benchmarks are in Appendix A.

Table 3: **Performance across different general video understanding/reasoning benchmarks.** * indicates our implementation performance.

Model	VideoMME		WorldSense		VideoMMMU		PerceptionTest
	Overall	Long	Overall	Recognition	Overall	Perception	Overall
<i>Proprietary Models</i>							
GPT-4o	71.9	-	42.6	-	61.2	66.0	-
<i>Tool-calling Methods</i>							
EgoR1	-	64.9	-	-	-	-	-
EgoR1 (w/o RAG)	58.7	50.8	42.0	40.3	34.4	37.6	65.8
LongVT-RL-7B	66.1	-	22.1	22.5	42.6	50.0	55.4
<i>Tool-free Methods</i>							
Qwen2.5-VL-7B	62.4	50.8	36.1	33.7	51.2	64.7	66.2
VideoRFT-7B	59.8	50.7	38.2	36.6	51.1	66.0	-
VideoR1-7B	61.4	50.6	35.5	32.8	52.4	65.3	-
Open-o3-video-7B	63.1*	53.1*	37.5	36.8	52.3	68.0	67.5
VISIONCOACH-7B (Ours)	63.3	53.2	43.8	41.8	54.4	70.3	68.7

4.2 Main Results

Results on V-STAR. We first evaluate the spatio-temporal reasoning capability of VISIONCOACH on V-STAR. As shown in Table 2, VISIONCOACH consistently outperforms both proprietary and open-source baselines across all evaluation dimensions. Compared to Qwen2.5-VL-7B, VISIONCOACH improves VQA accuracy by **+27.6** (33.5→61.1) and overall performance by **+15.0** mAM and **+25.1** mLGM. These results demonstrate that VISIONCOACH significantly strengthens grounded spatio-temporal reasoning, yielding consistent improvements in answer correctness, temporal localization, and spatial grounding, thereby validating the effectiveness of grounding-aware RL with self-distillation.

Results on general video understanding benchmarks. We compare the general video understanding capability of VISIONCOACH with GPT-4o, tool-calling models, and tool-free baselines. As shown in Table 3, VISIONCOACH consistently outperforms text-centric reasoning models (VideoR1 and VideoRFT) as well as tool-calling approaches, while remaining fully tool-free. Notably, VISIONCOACH shows substantial gains on perception-oriented categories, including WorldSense (Recognition) and VideoMMMU (Perception). These results indicate that improved spatio-temporal grounding not only enhances localization quality but also translates into stronger video answering.

Results on the temporal grounding benchmark. We evaluate VISIONCOACH on a temporal grounding benchmark and compare it against existing VideoLLMs specialized in temporal grounding. As shown in Table 4, VISIONCOACH consistently outperforms all competing methods. These results indicate that the proposed visual prompt guidance effectively facilitates the learning of accurate temporal grounding during training.

Results on the temporal grounding benchmark. We evaluate VISIONCOACH on a temporal grounding benchmark and compare it against existing VideoLLMs specialized in temporal grounding. As shown in Table 4, VISIONCOACH consistently outperforms all competing methods. These results indicate that the proposed visual prompt guidance effectively facilitates the learning of accurate temporal grounding during training.

4.3 Ablation Study

In this section, we conduct ablation studies to analyze the contribution of each component and key hyperparameters of VISIONCOACH. The default configuration is highlighted in yellow in the tables.

Ablation of VISIONCOACH. As shown in Table 5, we analyze the individual contribution of each component of VISIONCOACH on V-STAR using the spatio-temporal category subset of the STGR-RL dataset Meng et al. [2025]. We progressively enable four components: (i) the spatial grounding

Table 4: **Zero-shot temporal grounding performance on Charades-STA.**

	R@0.3	R@0.5	R@0.7	mIoU
<i>General Video LLMs</i>				
VideoChat	9.0	3.3	1.3	6.5
VideoLLaMA	10.4	3.8	0.9	7.1
Video-ChatGPT	20.0	7.7	1.7	13.7
Valley	28.4	1.8	0.3	21.4
<i>Temporal Grounding Video LLM</i>				
GroundingGPT	-	29.6	11.9	-
Momentor	42.6	26.6	11.6	28.5
TimeChat	-	32.2	13.4	-
HawkEye	50.6	31.4	14.5	33.7
VTG-LLM	51.2	33.8	15.7	34.4
VTimeLLM	51.0	27.5	11.4	31.2
<i>Grounded Reasoning Models</i>				
Open-o3-video	62.6	45.6	24.5	42.5
VISIONCOACH (Ours)	63.2	45.8	24.7	42.7

Table 5: **Ablation of VISIONCOACH on V-STAR.** r_{spa} : object-aware spatial grounding reward. \mathcal{L}_{SD} : self-distillation. VP-F: fixed visual prompting (darken). VP-S: VP-SELECTOR.

r_{spa}	\mathcal{L}_{SD}	VP-F	VP-S	Acc	mAM	mLGM
✓	-	-	-	59.4	31.1	42.7
✓	✓	-	-	59.6	30.4	41.6
✓	✓	darken	-	58.3	29.7	40.6
✓	✓	-	✓	60.7	31.3	43.1

Table 6: **VP-SELECTOR as plug-and-play module.** We evaluate the zero-shot performance of combining VP-SELECTOR with different reasoners.

Models	TVQA+ (In-domain)	PerceptionTest (Out-domain)
Qwen2.5-VL-7B +VP-SELECTOR	54.5 56.2	52.2 56.7
GPT-4o +VP-SELECTOR	71.8 75.3	61.5 62.4
Gemini-2.5-Flash +VP-SELECTOR	72.4 76.3	47.4 50.4

Table 7: **Ablation of hard sample threshold (k).**

k	Acc	mAM	mLGM
25%	57.0	29.7	40.0
50%	60.7	31.3	43.1
75%	59.7	29.8	41.3

Table 8: **Ablation of top- N self-distillation candidates.**

Top N	Acc	mAM	mLGM
Top 1	59.0	30.1	41.3
Top 2	60.7	31.3	43.1
Top 3	58.9	29.2	40.2

Table 9: **Ablation of overall reward combination.**

r_{fmt}	r_{acc}	r_{tmp}	r_{spa}	Acc	mAM	mLGM
✓	-	✓	✓	56.9	29.5	39.8
✓	✓	✓	-	58.5	29.4	40.3
✓	✓	✓	✓	60.7	31.3	43.1

reward (r_{spa}), (ii) the self-distillation loss (\mathcal{L}_{SD}), (iii) fixed visual prompting (VP-F; Darken), and (iv) VP-SELECTOR (VP-S). Specifically, self-distillation alone slightly improves VQA accuracy (59.4 \rightarrow 59.6) but reduces grounding performance (mAM 31.1 \rightarrow 30.4), while fixed visual prompting further degrades grounding. In contrast, combining input-adaptive prompting with self-distillation achieves the best performance across all metrics, demonstrating that selectively applying prompts provides effective grounding guidance while avoiding unnecessary perturbations. Moreover, as shown in Figure 4 (c), models trained with VP guidance achieve consistently higher reward values and faster early-stage improvement during training, indicating that VP provides informative signals that encourage attention to question-relevant regions. Additional ablation studies are in Appendix D.

Ablation of hard sample threshold. Since VISIONCOACH selects hard samples based on a reward threshold, we analyze the effect of different threshold values in Table 7. We determine the threshold based on the reward distribution of Open-o3-video Meng et al. [2025] and set the mean reward as the default threshold. As shown in Table 7, using a moderate threshold ($k = 50\%$) achieves the best performance across all metrics. Lower thresholds include many relatively easy samples, providing weaker supervision, while overly high thresholds reduce the number of selected samples and limit effective training signals. These results suggest that selecting a balanced set of sufficiently challenging samples is important for effective training.

Ablation of top- N self-distillation candidates. As shown in Table 8, we analyze the effect of the number of trajectories used for self-distillation. Selecting the top-2 candidates achieves the best performance across all metrics, while using only the top-1 candidate leads to slightly lower improvements due to reduced supervision signals. However, increasing the number of candidates to top-3 degrades performance. We hypothesize that including more candidates introduces *lower-quality* reasoning trajectories into the distillation objective, which dilutes the supervision signal from the highest-reward trajectories. As a result, the model may imitate suboptimal reasoning behaviors, weakening the benefits of self-distillation. It suggests that distilling a small set of high-quality trajectories provides a better balance between stable supervision and avoiding noisy imitation.

Ablation of overall reward design. As shown in Table 9, we ablate each reward component to analyze its individual effect. Starting from the combination of format reward, temporal reward, and spatial reward (first row), adding answer reward improves all metrics, increasing accuracy from 56.9 to 58.5 while also improving grounding performance. Further incorporating all reward components yields the best overall results, achieving 60.7 Acc, 31.3 mAM, and 43.1 mLGM. These results show that each reward contributes complementary supervision, and that jointly optimizing answer correctness and grounded spatio-temporal reasoning is crucial for strong performance.

Statistics of adaptive visual prompting. To better understand the behavior of VISIONCOACH’s adaptive visual prompting mechanism, we analyze the distribution of designated sample difficulty

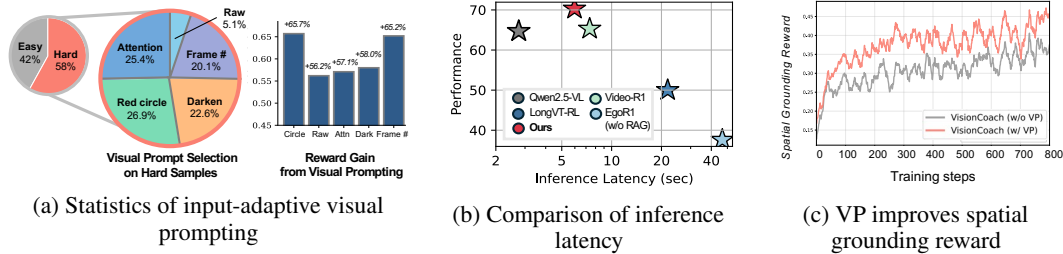


Figure 4: **More analysis of VISIONCOACH.** We provide analysis including (a) statistics of visual prompting, (b) inference latency, and (c) the effect of visual prompting on spatial grounding reward.

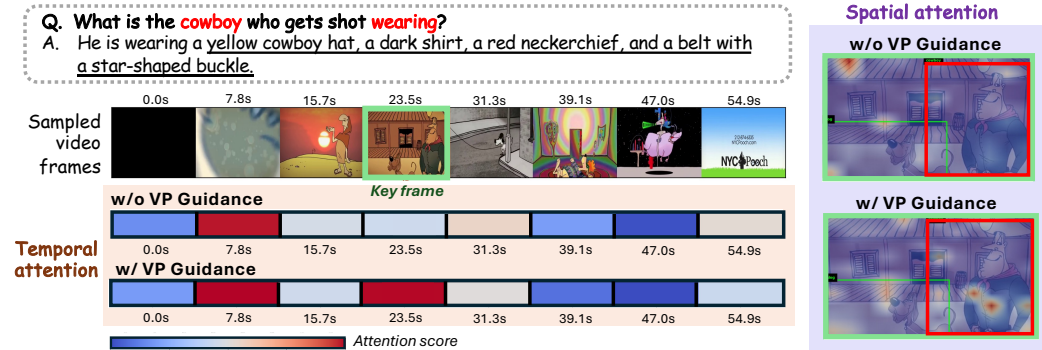


Figure 5: **Spatio-temporal attention map.** Visual prompting (VP) improves grounding in both temporal and spatial dimensions. The green box indicates the key frame, while the red box highlights the corresponding spatial region. Temporally, VP increases attention on the correct key frame containing the cowboy. Spatially, VP concentrates attention on the region corresponding to the queried visual attributes (e.g., the cowboy wearing specific clothing), while suppressing irrelevant regions.

(Easy vs. Hard), the visual prompts selected for hard samples by VP-SELECTOR, and the resulting reward gain from each prompt. We compute the relative reward gain as $(R'_i - \bar{R}_i) / \bar{R}_i \times 100$. As shown in Figure 4 (a), 58% of the samples are identified as hard. For these hard samples, VP-SELECTOR dynamically chooses among multiple visual prompting types. Applying these prompts consistently leads to reward improvements, with gains ranging from +56% to +66% across different prompt types. It indicates that visual prompting provides effective guidance for challenging instances, and the VP-SELECTOR identifies visual prompts that yield meaningful training signals.

VP-SELECTOR as a plug-and-play module. As shown in Table 6, we evaluate VP-SELECTOR as a standalone module by integrating it with various MLLM backbones to augment video inputs prior to reasoning. We conduct experiments on the TVQA+ validation set (in-domain) and on a uniformly sampled subset from each category of the PerceptionTest validation set (out-of-domain). Incorporating VP-SELECTOR consistently improves performance across different backbone models on both benchmarks. These results demonstrate that VP-SELECTOR functions as a plug-and-play module for enhancing grounded visual reasoning.

4.4 More Analysis

Inference latency. To evaluate per-sample inference latency, we measure runtime on a single NVIDIA RTX 6000 (40GB) GPU and compare text-centric reasoning, tool-calling reasoning, and VISIONCOACH. As shown in Figure 4 (b), VISIONCOACH consistently outperforms both text-centric (Qwen2.5-VL, Video-R1) and tool-calling (EgoR1, LongVT-RL) baselines while operating at substantially lower inference latency than external tool-based approaches.

Spatio-temporal attention map. To examine how visual prompting facilitates spatio-temporal grounding during training, we analyze the attention maps from the last layer of VISIONCOACH. Specifically, we compute the average attention across all heads and measure the attention scores between the question tokens and visual tokens. Temporal attention is aggregated at the frame level,

while spatial attention is aggregated over patch-level regions within each frame. As illustrated in Figure 5, without VP guidance, both spatial and temporal attention are broadly dispersed across irrelevant frames and background regions, resulting in weak localization of the question-relevant event. In contrast, with VP guidance, the model concentrates attention on the key frame where the cowboy is shot and focuses on semantically relevant regions, such as the character and surrounding objects. This comparison indicates that VP guidance promotes more accurate temporal localization and spatial grounding, enabling better alignment between reasoning and visual evidence. Additional analyses, including qualitative examples, reward ablations, and limitations are provided in the Appendix D.

5 Conclusion

In this work, we introduced VISIONCOACH, an instance-adaptive RL framework for grounded video reasoning. VISIONCOACH applies visual prompting during RL to explicitly expose question-relevant evidence during learning using VP-SELECTOR and ST-REASONER. For hard example, VP-SELECTOR predicts appropriate prompting strategies, and ST-REASONER internalizes these signals through RL-based self-distillation, enabling the model to learn grounded reasoning behaviors. We further design object-aware spatial grounding rewards that enforce object identity consistency and multi-region spatial alignment, encouraging accurate multi-object reasoning beyond answer-only supervision. Experiments across multiple challenging benchmarks across tasks show consistent gains in both reasoning and grounding accuracy, while preserving a single, efficient inference pathway.

Acknowledgement

This work was supported by ONR Grant N00014-23-1-2356, ARO Award W911NF2110220, DARPA ECOLE Program No. HR00112390060, and NSF-AI Engage Institute DRL2112635. The views contained in this article are those of the authors and not of the funding agency.

References

- Lisa Anne Hendricks, Oliver Wang, Eli Shechtman, Josef Sivic, Trevor Darrell, and Bryan Russell. Localizing moments in video with natural language. In *Proceedings of the IEEE international conference on computer vision*, pages 5803–5812, 2017.
- Shuai Bai, Yuxuan Cai, Ruizhe Chen, Keqin Chen, Xionghui Chen, Zesen Cheng, Lianghao Deng, Wei Ding, Chang Gao, Chunjiang Ge, et al. Qwen3-vl technical report. *arXiv preprint arXiv:2511.21631*, 2025a.
- Shuai Bai, Keqin Chen, Xuejing Liu, Jialin Wang, Wenbin Ge, Sibao Song, Kai Dang, Peng Wang, Shijie Wang, Jun Tang, et al. Qwen2. 5-vl technical report. corr, abs/2502.13923, 2025. doi: 10.48550. *arXiv preprint 2502.13923*, 2025b.
- Fabian Caba Heilbron, Victor Escorcia, Bernard Ghanem, and Juan Carlos Niebles. Activitynet: A large-scale video benchmark for human activity understanding. In *Proceedings of the IEEE conference on computer vision and pattern recognition*, pages 961–970, 2015.
- Mu Cai, Haotian Liu, Siva Karthik Mustikovela, Gregory P Meyer, Yuning Chai, Dennis Park, and Yong Jae Lee. Vip-llava: Making large multimodal models understand arbitrary visual prompts. pages 12914–12923, 2024.
- Ruizhe Chen, Tianze Luo, Zhiting Fan, Heqing Zou, Zhaopeng Feng, Guiyang Xie, Hansheng Zhang, Zhuochen Wang, Zuozhu Liu, and Zhang Huaijian. Datasets and recipes for video temporal grounding via reinforcement learning. In *Proceedings of the 2025 Conference on Empirical Methods in Natural Language Processing: Industry Track*, pages 983–992, 2025a.
- Yukang Chen, Wei Huang, Baifeng Shi, Qinghao Hu, Hanrong Ye, Ligeng Zhu, Zhijian Liu, Pavlo Molchanov, Jan Kautz, Xiaojuan Qi, et al. Scaling rl to long videos. *arXiv preprint arXiv:2507.07966*, 2025b.

- Zhe Chen, Jiannan Wu, Wenhai Wang, Weijie Su, Guo Chen, Sen Xing, Muyan Zhong, Qinglong Zhang, Xizhou Zhu, Lewei Lu, et al. Internvl: Scaling up vision foundation models and aligning for generic visual-linguistic tasks. In *Proceedings of the IEEE/CVF Conference on Computer Vision and Pattern Recognition*, pages 24185–24198, 2024.
- Junhao Cheng, Yuying Ge, Teng Wang, Yixiao Ge, Jing Liao, and Ying Shan. Video-holmes: Can mllm think like holmes for complex video reasoning? *arXiv preprint arXiv:2505.21374*, 2025a.
- Zixu Cheng, Jian Hu, Ziquan Liu, Chenyang Si, Wei Li, and Shaogang Gong. V-star: Benchmarking video-llms on video spatio-temporal reasoning. *arXiv preprint arXiv:2503.11495*, 2025b.
- Zixu Cheng, Da Li, Jian Hu, Ziquan Liu, Wei Li, and Shaogang Gong. Graphthinker: Reinforcing video reasoning with event graph thinking. *arXiv preprint arXiv:2602.17555*, 2026.
- Jang Hyun Cho, Andrea Madotto, Effrosyni Mavroudi, Triantafyllos Afouras, Tushar Nagarajan, Muhammad Maaz, Yale Song, Tengyu Ma, Shuming Hu, Suyog Jain, et al. Perceptionlm: Open-access data and models for detailed visual understanding. *arXiv preprint arXiv:2504.13180*, 2025.
- Rohan Choudhury, Koichiro Niinuma, Kris M Kitani, and László A Jeni. Video question answering with procedural programs. In *European Conference on Computer Vision*, pages 315–332. Springer, 2024.
- Gheorghe Comanici, Eric Bieber, Mike Schaekermann, Ice Pasupat, Noveen Sachdeva, Inderjit Dhillon, Marcel Blistein, Ori Ram, Dan Zhang, Evan Rosen, et al. Gemini 2.5: Pushing the frontier with advanced reasoning, multimodality, long context, and next generation agentic capabilities. *arXiv preprint arXiv:2507.06261*, 2025.
- Andong Deng, Tongjia Chen, Shoubin Yu, Taojiannan Yang, Lincoln Spencer, Yapeng Tian, Ajmal Saeed Mian, Mohit Bansal, and Chen Chen. Motion-grounded video reasoning: Understanding and perceiving motion at pixel level. In *Proceedings of the Computer Vision and Pattern Recognition Conference*, pages 8625–8636, 2025a.
- Andong Deng, Taojiannan Yang, Shoubin Yu, Lincoln Spencer, Mohit Bansal, Chen Chen, Serena Yeung-Levy, and Xiaohan Wang. Scivideobench: Benchmarking scientific video reasoning in large multimodal models. *arXiv preprint arXiv:2510.08559*, 2025b.
- Andong Deng, Taojiannan Yang, Shoubin Yu, Lincoln Spencer, Mohit Bansal, Chen Chen, Serena Yeung-Levy, and Xiaohan Wang. Scivideobench: Benchmarking scientific video reasoning in large multimodal models. *arXiv preprint arXiv:2510.08559*, 2025c.
- Kaituo Feng, Kaixiong Gong, Bohao Li, Zonghao Guo, Yibing Wang, Tianshuo Peng, Junfei Wu, Xiaoying Zhang, Benyou Wang, and Xiangyu Yue. Video-r1: Reinforcing video reasoning in mllms. *arXiv preprint arXiv:2503.21776*, 2025.
- Chaoyou Fu, Yuhan Dai, Yongdong Luo, Lei Li, Shuhuai Ren, Renrui Zhang, Zihan Wang, Chenyu Zhou, Yunhang Shen, Mengdan Zhang, et al. Video-mme: The first-ever comprehensive evaluation benchmark of multi-modal llms in video analysis. In *Proceedings of the Computer Vision and Pattern Recognition Conference*, pages 24108–24118, 2025.
- Tommaso Furlanello, Zachary Lipton, Michael Tschannen, Laurent Itti, and Anima Anandkumar. Born again neural networks. In *International conference on machine learning*, pages 1607–1616. PMLR, 2018.
- Jiyang Gao, Chen Sun, Zhenheng Yang, and Ram Nevatia. Tall: Temporal activity localization via language query. In *Proceedings of the IEEE international conference on computer vision*, pages 5267–5275, 2017.
- Haonan Ge, Yiwei Wang, Kai-Wei Chang, Hang Wu, and Yujun Cai. Framemind: Frame-interleaved video reasoning via reinforcement learning. *arXiv preprint arXiv:2509.24008*, 2025.
- Google DeepMind. Gemini 2 technical report, 2025. URL <https://deepmind.google/technologies/gemini/>.

- Xin Gu, Haoji Zhang, Qihang Fan, Jingxuan Niu, Zhipeng Zhang, Libo Zhang, Guang Chen, Fan Chen, Longyin Wen, and Sijie Zhu. Thinking with bounding boxes: Enhancing spatio-temporal video grounding via reinforcement fine-tuning. *arXiv preprint arXiv:2511.21375*, 2025.
- Daya Guo, Dejian Yang, Haowei Zhang, Junxiao Song, Ruoyu Zhang, Runxin Xu, Qihao Zhu, Shirong Ma, Peiyi Wang, Xiao Bi, et al. Deepseek-r1: Incentivizing reasoning capability in llms via reinforcement learning. *arXiv preprint arXiv:2501.12948*, 2025.
- Yongxin Guo, Jingyu Liu, Mingda Li, Qingbin Liu, Xi Chen, and Xiaoying Tang. Trace: Temporal grounding video llm via causal event modeling. *arXiv preprint arXiv:2410.05643*, 2024.
- Songhao Han, Wei Huang, Hairong Shi, Le Zhuo, Xiu Su, Shifeng Zhang, Xu Zhou, Xiaojuan Qi, Yue Liao, and Si Liu. Videoespresso: A large-scale chain-of-thought dataset for fine-grained video reasoning via core frame selection. In *Proceedings of the Computer Vision and Pattern Recognition Conference*, pages 26181–26191, 2025.
- Geoffrey Hinton, Oriol Vinyals, and Jeff Dean. Distilling the knowledge in a neural network. 2015.
- Jack Hong, Shilin Yan, Jiayin Cai, Xiaolong Jiang, Yao Hu, and Weidi Xie. Worldsense: Evaluating real-world omnimodal understanding for multimodal llms. *arXiv preprint arXiv:2502.04326*, 2025a.
- Jack Hong, Shilin Yan, Jiayin Cai, Xiaolong Jiang, Yao Hu, and Weidi Xie. Worldsense: Evaluating real-world omnimodal understanding for multimodal llms. *arXiv preprint arXiv:2502.04326*, 2025b.
- Edward J Hu, Yelong Shen, Phillip Wallis, Zeyuan Allen-Zhu, Yuanzhi Li, Shean Wang, Liang Wang, Weizhu Chen, et al. Lora: Low-rank adaptation of large language models. *Iclr*, 1(2):3, 2022.
- Kairui Hu, Penghao Wu, Fanyi Pu, Wang Xiao, Yuanhan Zhang, Xiang Yue, Bo Li, and Ziwei Liu. Video-mmmu: Evaluating knowledge acquisition from multi-discipline professional videos. *arXiv preprint arXiv:2501.13826*, 2025.
- Aaron Hurst, Adam Lerer, Adam P Goucher, Adam Perelman, Aditya Ramesh, Aidan Clark, AJ Ostrow, Akila Welihinda, Alan Hayes, Alec Radford, et al. Gpt-4o system card. *arXiv preprint arXiv:2410.21276*, 2024.
- Daeyeon Lee, Jaehong Yoon, Jaemin Cho, and Mohit Bansal. Video-skill-cot: Skill-based chain-of-thoughts for domain-adaptive video reasoning. *arXiv preprint arXiv:2506.03525*, 2025.
- Jie Lei, Licheng Yu, Tamara Berg, and Mohit Bansal. Tvqa+: Spatio-temporal grounding for video question answering. In *Proceedings of the 58th annual meeting of the association for computational linguistics*, pages 8211–8225, 2020.
- Jie Lei, Tamara L Berg, and Mohit Bansal. Detecting moments and highlights in videos via natural language queries. *Advances in Neural Information Processing Systems*, 34:11846–11858, 2021.
- Bo Li, Yuanhan Zhang, Dong Guo, Renrui Zhang, Feng Li, Hao Zhang, Kaichen Zhang, Peiyuan Zhang, Yanwei Li, Ziwei Liu, et al. Llava-onevision: Easy visual task transfer. *arXiv preprint arXiv:2408.03326*, 2024a.
- Feng Li, Qing Jiang, Hao Zhang, Tianhe Ren, Shilong Liu, Xueyan Zou, Huaizhe Xu, Hongyang Li, Jianwei Yang, Chunyuan Li, et al. Visual in-context prompting. pages 12861–12871, 2024b.
- Junnan Li, Dongxu Li, Silvio Savarese, and Steven Hoi. Blip-2: Bootstrapping language-image pre-training with frozen image encoders and large language models. In *International conference on machine learning*, pages 19730–19742. PMLR, 2023.
- Kunchang Li, Yali Wang, Yinan He, Yizhuo Li, Yi Wang, Yi Liu, Zun Wang, Jilan Xu, Guo Chen, Ping Luo, et al. Mvbench: A comprehensive multi-modal video understanding benchmark. In *Proceedings of the IEEE/CVF Conference on Computer Vision and Pattern Recognition*, pages 22195–22206, 2024c.

- Xinhao Li, Ziang Yan, Desen Meng, Lu Dong, Xiangyu Zeng, Yinan He, Yali Wang, Yu Qiao, Yi Wang, and Limin Wang. Videochat-r1: Enhancing spatio-temporal perception via reinforcement fine-tuning. *arXiv preprint arXiv:2504.06958*, 2025.
- Aixin Liu, Bei Feng, Bing Xue, Bingxuan Wang, Bochao Wu, Chengda Lu, Chenggang Zhao, Chengqi Deng, Chenyu Zhang, Chong Ruan, et al. Deepseek-v3 technical report. *arXiv preprint arXiv:2412.19437*, 2024a.
- Zuyan Liu, Yuhao Dong, Ziwei Liu, Winston Hu, Jiwen Lu, and Yongming Rao. Oryx mllm: On-demand spatial-temporal understanding at arbitrary resolution. *arXiv preprint arXiv:2409.12961*, 2024b.
- Jiahao Meng, Xiangtai Li, Haochen Wang, Yue Tan, Tao Zhang, Lingdong Kong, Yunhai Tong, Anran Wang, Zhiyang Teng, Yujing Wang, et al. Open-o3 video: Grounded video reasoning with explicit spatio-temporal evidence. *arXiv preprint arXiv:2510.20579*, 2025.
- Andreea-Maria Oncescu, Joao F Henriques, Yang Liu, Andrew Zisserman, and Samuel Albanie. Queryd: A video dataset with high-quality text and audio narrations. In *ICASSP 2021-2021 IEEE International Conference on Acoustics, Speech and Signal Processing (ICASSP)*, pages 2265–2269. IEEE, 2021.
- Viorica Patraucean, Lucas Smaira, Ankush Gupta, Adria Recasens, Larisa Markeeva, Dylan Banarse, Skanda Koppula, Mateusz Malinowski, Yi Yang, Carl Doersch, et al. Perception test: A diagnostic benchmark for multimodal video models. *Advances in Neural Information Processing Systems*, 36: 42748–42761, 2023.
- Hanoona Rasheed, Mohammed Zumri, Muhammad Maaz, Ming-Hsuan Yang, Fahad Shahbaz Khan, and Salman Khan. Video-com: Interactive video reasoning via chain of manipulations. *arXiv preprint arXiv:2511.23477*, 2025.
- Shuhuai Ren, Linli Yao, Shicheng Li, Xu Sun, and Lu Hou. Timechat: A time-sensitive multimodal large language model for long video understanding. In *Proceedings of the IEEE/CVF Conference on Computer Vision and Pattern Recognition*, pages 14313–14323, 2024.
- Andrei A Rusu, Sergio Gomez Colmenarejo, Caglar Gulcehre, Guillaume Desjardins, James Kirkpatrick, Razvan Pascanu, Volodymyr Mnih, Koray Kavukcuoglu, and Raia Hadsell. Policy distillation. *arXiv preprint arXiv:1511.06295*, 2015.
- Hao Shao, Shengju Qian, Han Xiao, Guanglu Song, Zhuofan Zong, Letian Wang, Yu Liu, and Hongsheng Li. Visual cot: Advancing multi-modal language models with a comprehensive dataset and benchmark for chain-of-thought reasoning. *Advances in Neural Information Processing Systems*, 37:8612–8642, 2024.
- Aleksandar Shtedritski, Christian Rupprecht, and Andrea Vedaldi. What does clip know about a red circle? visual prompt engineering for vlms. pages 11987–11997, 2023.
- Yansong Tang, Dajun Ding, Yongming Rao, Yu Zheng, Danyang Zhang, Lili Zhao, Jiwen Lu, and Jie Zhou. Coin: A large-scale dataset for comprehensive instructional video analysis. In *Proceedings of the IEEE/CVF Conference on Computer Vision and Pattern Recognition*, pages 1207–1216, 2019.
- Shulin Tian, Ruiqi Wang, Hongming Guo, Penghao Wu, Yuhao Dong, Xiuying Wang, Jingkang Yang, Hao Zhang, Hongyuan Zhu, and Ziwei Liu. Ego-r1: Chain-of-tool-thought for ultra-long egocentric video reasoning. *arXiv preprint arXiv:2506.13654*, 2025.
- Haochen Wang, Xiangtai Li, Zilong Huang, Anran Wang, Jiacong Wang, Tao Zhang, Jiani Zheng, Sule Bai, Zijian Kang, Jiashi Feng, et al. Traceable evidence enhanced visual grounded reasoning: Evaluation and methodology. *arXiv preprint arXiv:2507.07999*, 2025a.
- Qi Wang, Yanrui Yu, Ye Yuan, Rui Mao, and Tianfei Zhou. Videort: Incentivizing video reasoning capability in mllms via reinforced fine-tuning. *arXiv preprint arXiv:2505.12434*, 2025b.

- Ye Wang, Ziheng Wang, Boshen Xu, Yang Du, Kejun Lin, Zihan Xiao, Zihao Yue, Jianzhong Ju, Liang Zhang, Dingyi Yang, et al. Time-r1: Post-training large vision language model for temporal video grounding. *arXiv preprint arXiv:2503.13377*, 2025c.
- Ziyang Wang, Jaehong Yoon, Shoubin Yu, Md Mohaiminul Islam, Gedas Bertasius, and Mohit Bansal. Video-rts: Rethinking reinforcement learning and test-time scaling for efficient and enhanced video reasoning. In *Proceedings of the 2025 Conference on Empirical Methods in Natural Language Processing*, pages 28114–28128, 2025d.
- Bo Wu, Shoubin Yu, Zhenfang Chen, Joshua B Tenenbaum, and Chuang Gan. Star: A benchmark for situated reasoning in real-world videos. *arXiv preprint arXiv:2405.09711*, 2024a.
- Junda Wu, Zhehao Zhang, Yu Xia, Xintong Li, Zhaoyang Xia, Aaron Chang, Tong Yu, Sungchul Kim, Ryan A Rossi, Ruiyi Zhang, et al. Visual prompting in multimodal large language models: A survey. *arXiv preprint arXiv:2409.15310*, 2024b.
- Yongliang Wu, Xinting Hu, Yuyang Sun, Yizhou Zhou, Wenbo Zhu, Fengyun Rao, Bernt Schiele, and Xu Yang. Number it: Temporal grounding videos like flipping manga. *arXiv preprint arXiv:2411.10332*, 2024c.
- Ziang Yan, Xinhao Li, Yinan He, Zhengrong Yue, Xiangyu Zeng, Yali Wang, Yu Qiao, Limin Wang, and Yi Wang. Videochat-r1.5: Visual test-time scaling to reinforce multimodal reasoning by iterative perception. *arXiv preprint arXiv:2509.21100*, 2025.
- Zuhao Yang, Sudong Wang, Kaichen Zhang, Keming Wu, Sicong Leng, Yifan Zhang, Bo Li, Chengwei Qin, Shijian Lu, Xingxuan Li, et al. Longvt: Incentivizing "thinking with long videos" via native tool calling. *arXiv preprint arXiv:2511.20785*, 2025.
- Runpeng Yu, Weihao Yu, and Xinchao Wang. Attention prompting on image for large vision-language models. In *European Conference on Computer Vision*, pages 251–268. Springer, 2024.
- Shoubin Yu, Yue Zhang, Zun Wang, Jaehong Yoon, Huaxiu Yao, Mingyu Ding, and Mohit Bansal. When and how much to imagine: Adaptive test-time scaling with world models for visual spatial reasoning. *arXiv preprint arXiv:2602.08236*, 2026.
- Xiangyu Zeng, Zhiqiu Zhang, Yuhan Zhu, Xinhao Li, Zikang Wang, Changlian Ma, Qingyu Zhang, Zizheng Huang, Kun Ouyang, Tianxiang Jiang, et al. Video-o3: Native interleaved clue seeking for long video multi-hop reasoning. *arXiv preprint arXiv:2601.23224*, 2026.
- Boqiang Zhang, Kehan Li, Zesen Cheng, Zhiqiang Hu, Yuqian Yuan, Guanzheng Chen, Sicong Leng, Yuming Jiang, Hang Zhang, Xin Li, et al. Videollama 3: Frontier multimodal foundation models for image and video understanding. *arXiv preprint arXiv:2501.13106*, 2025a.
- Haoji Zhang, Xin Gu, Jiawen Li, Chixiang Ma, Sule Bai, Chubin Zhang, Bowen Zhang, Zhichao Zhou, Dongliang He, and Yansong Tang. Thinking with videos: Multimodal tool-augmented reinforcement learning for long video reasoning. *arXiv preprint arXiv:2508.04416*, 2025b.
- Jinglei Zhang, Yuanfan Guo, Rolandos Alexandros Potamias, Jiankang Deng, Hang Xu, and Chao Ma. Vtimecot: Thinking by drawing for video temporal grounding and reasoning. In *Proceedings of the IEEE/CVF International Conference on Computer Vision*, pages 24203–24213, 2025c.
- Yichi Zhang, Yinpeng Dong, Siyuan Zhang, Tianzan Min, Hang Su, and Jun Zhu. Exploring the transferability of visual prompting for multimodal large language models. pages 26562–26572, 2024a.
- Yuan Zhang, Chun-Kai Fan, Tao Huang, Ming Lu, Sicheng Yu, Junwen Pan, Kuan Cheng, Qi She, and Shanghang Zhang. Autov: Learning to retrieve visual prompt for large vision-language models. *arXiv preprint arXiv:2506.16112*, 2025d.
- Yuan Zhang, Chun-Kai Fan, Tao Huang, Ming Lu, Sicheng Yu, Junwen Pan, Kuan Cheng, Qi She, and Shanghang Zhang. Autov: Learning to retrieve visual prompt for large vision-language models. *arXiv e-prints*, pages arXiv–2506, 2025e.

Yuanhan Zhang, Jinming Wu, Wei Li, Bo Li, Zejun Ma, Ziwei Liu, and Chunyuan Li. Llava-video: Video instruction tuning with synthetic data. *arXiv preprint arXiv:2410.02713*, 2024b.

Chujie Zheng, Shixuan Liu, Mingze Li, Xiong-Hui Chen, Bowen Yu, Chang Gao, Kai Dang, Yuqiong Liu, Rui Men, An Yang, et al. Group sequence policy optimization. *arXiv preprint arXiv:2507.18071*, 2025.

Appendix

A Evaluation Details	1
A.1 Baselines	1
A.2 Evaluation Metrics	1
B Implementation Details of VISIONCOACH	2
B.1 Training Datasets	2
B.2 More Training and Inference Details	2
C Details of VP-SELECTOR	3
C.1 Details of Visual Prompting Types	3
C.2 Data Collection	3
C.3 Data Statistics	4
C.4 Model Architecture	4
D Additional Analysis	4
D.1 Ablation of Hyperparameter	5
D.2 Ablation of Reward	5
D.3 Ablation of Visual Prompting Assignment	6
E Visualization	6
F Limitation and Future Work	7

A Evaluation Details

A.1 Baselines

We compare VISIONCOACH with proprietary models (GPT-4o and Gemini-2.0-Flash) and open-source models including Video-LLaMA3 Zhang et al. [2025a], LLaVA-Video, and Open-o3-video Meng et al. [2025]. We further include text-based reasoning models (VideoR1 Feng et al. [2025], VideoRFT Wang et al. [2025b]), tool-calling models (Ego-R1-3B Tian et al. [2025] with GPT-4o and Gemini-2.0-Flash, and LongVT-RL-7B Yang et al. [2025]), and temporal grounding Video LLMs such as TimeChat Ren et al. [2024]. For Ego-R1 Tian et al. [2025], to enable evaluation across diverse benchmarks, we disable its dataset-specific RAG tools and retain the remaining tools.

A.2 Evaluation Metrics

V-STAR benchmark. We evaluate VISIONCOACH’s spatio-temporal grounding reasoning ability using the V-STAR Cheng et al. [2025b] benchmark. V-STAR decomposes video reasoning into fine-grained Chain-of-Thought (CoT) questions along three dimensions: *what*, *when*, and *where*. Chain1 corresponds to the reasoning order *what–when–where*, while Chain2 follows *what–where–when*. Each dimension is evaluated using dedicated metrics: answer accuracy (Acc), mean temporal IoU (m_tIoU), and mean visual IoU (m_vIoU), respectively. To measure the overall reasoning performance across these dimensions, V-STAR first aggregates the three metrics using the Arithmetic Mean (AM) and Geometric Mean (GM):

$$AM = \frac{1}{3}(Acc + m_tIoU + m_vIoU) \quad (9)$$

$$GM = (Acc \times m_tIoU \times m_vIoU)^{\frac{1}{3}} \quad (10)$$

However, when any metric becomes zero, GM collapses to zero. To mitigate this issue, the benchmark adopts a logarithmic transformation and defines the Logarithmic Geometric Mean (LGM):

$$LGM = -\frac{1}{3} [\ln(1 - Acc + \epsilon) + \ln(1 - m_tIoU + \epsilon) + \ln(1 - m_vIoU + \epsilon)] \quad (11)$$

where ϵ is a small constant preventing $\ln(0)$ when any metric approaches 1. Since the same questions can appear in different CoT chains, the benchmark further computes the mean AM (mAM) and mean LGM (mLGM) across chains:

$$mAM = \frac{1}{n} \sum_{k=1}^n AM_k, \quad mLGM = \frac{1}{n} \sum_{k=1}^n LGM_k \quad (12)$$

where n denotes the number of reasoning chains. The mAM and mLGM metrics therefore capture the model’s overall spatio-temporal reasoning performance across different reasoning orders.

General video understanding benchmark. For all video understanding benchmark including VideoMME Fu et al. [2025], WorldSense Hong et al. [2025b], VideoMMMU Hu et al. [2025], and PerceptionTest Patraucean et al. [2023], we report multi-choice question accuracy.

Temporal grounding benchmark. We evaluate temporal grounding performance using standard metrics on Charades-STA Gao et al. [2017]. Given a predicted temporal segment and the ground-truth interval for each query, we compute temporal Intersection over Union (tIoU) between the two segments. We report Recall at different IoU thresholds, including R@0.3, R@0.5, and R@0.7, which measure the percentage of queries whose predicted segment achieves a tIoU greater than the specified threshold. We also report mean IoU (mIoU), defined as the average temporal IoU across all queries.

B Implementation Details of VISIONCOACH

B.1 Training Datasets

In this section, we provide details for each SFT and RL stage.

Cold-start initialization. We use STGR-CoT-30k Meng et al. [2025] dataset for SFT-based cold-start initialization. This dataset is composed of four parts: (i) 4.1k temporal grounding chain-of-thought samples from TVG-ColdStart Chen et al. [2025a], (ii) 5k spatial grounding samples from TreeVGR-SFT Wang et al. [2025a], (iii) 5.9k spatio-temporal samples curated from multiple video sources, including 3.9k samples from temporal grounding datasets such as ActivityNet Caba Heilbron et al. [2015], COIN Tang et al. [2019], QueryD Oncescu et al. [2021], QVHighlight Lei et al. [2021], and DiDeMo Anne Hendricks et al. [2017], together with 2k samples from PLM-Rdcap Cho et al. [2025], and (iv) 15k video reasoning samples from Video-R1-CoT Feng et al. [2025].

Reinforcement learning. For RL, we train on the STGR-RL-36k dataset Meng et al. [2025], which further increases the diversity of grounding scenarios. The dataset contains four components: (i) 5.2k temporal grounding samples, including 2.3k from Time-R1 Wang et al. [2025c] and 2.9k from TVG-RL Chen et al. [2025a], (ii) 5k spatial grounding samples from VisCoT Shao et al. [2024], (iii) 10.9k spatio-temporal samples consisting of the 5.9k samples from Open-o3-video Meng et al. [2025] and 5k filtered samples from VideoEspresso Han et al. [2025], and (iv) 15k video reasoning samples from Video-R1 Feng et al. [2025].

B.2 More Training and Inference Details

We uniformly sample 16 frames from each video as input. For both cold-start and RL stage, we use one epoch with a learning rate of 1×10^{-6} . Unless otherwise specified, we use 8 NVIDIA GPUs with DeepSpeed ZeRO-3 optimization, a per-device batch size of 1, and gradient accumulation steps of 1. We set the maximum prompt length and completion length to 16,384 and 768 tokens, respectively. For GSPO training, we sample 4 rollouts per input and set the KL coefficient β to 0.04. We use a cosine learning rate scheduler, weight decay of 0.01, and gradient clipping with a maximum norm of

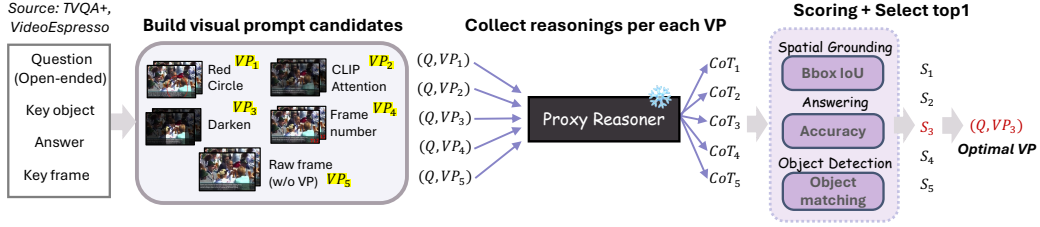


Figure 6: **VP-SELECTOR training data generation pipeline.** Given a video-question pair, we construct multiple visual prompting candidates, generate grounded reasoning with proxy reasoners, and derive pseudo-labels for selecting the most effective visual prompt.

5. For VISIONCOACH, we empirically set the hard-question threshold to $k = 2.21$, which means Open-o3-video’s average number of rewards. We use the average of r_{spa} , r_{tmp} , and r_{acc} to select self-distillation candidates C_i and only use r_{acc} to select the top 2 self-distilled examples.

C Details of VP-SELECTOR

C.1 Details of Visual Prompting Types

In this section, we provide details of each visual prompting type. We also include raw frames without visual prompting, as visual guidance is not always beneficial Yu et al. [2024], Zhang et al. [2025e].

Key-object-based visual prompting (Darken/Red circle). We construct key-object-based visual prompts using object GT bounding boxes. For the red circle, we draw a circle centered at the bounding box center with a radius covering the object region to explicitly highlight the target object, following Shtedritski et al. [2023]. For the darken, we darken the regions outside the bounding boxes while preserving the object area, thereby guiding the model’s attention to the relevant object.

Frame numbering. To provide explicit temporal cues, we overlay frame indices on each video frame following Wu et al. [2024c]. The key frame index is rendered as a red numeric label at the bottom-right corner.

Attention-based prompt. Following API prompting Yu et al. [2024], we generate attention-based visual prompts using CLIP-ViT-L-14-336 by computing a query-conditioned spatial relevance map for each key frame. Visual features from an intermediate CLIP layer are projected onto the text embedding to obtain relevance maps, which are normalized and blended with the input frame to highlight query-relevant regions.

C.2 Data Collection

We illustrate our data collection pipeline in Figure 6. Given a video-question pair, we construct multiple visual prompting candidates, generate grounded reasoning with proxy reasoners, and derive pseudo-labels for selecting the most effective visual prompt.

Proxy reasoner. For each visual prompting candidate constructed above based on TVQA+ Lei et al. [2020] and VideoEspresso Han et al. [2025] training dataset, we generate grounded reasoning trajectories using multiple proxy reasoners, including Qwen3-VL-30B Bai et al. [2025a], Gemini-2.5-Flash Google DeepMind [2025], and GPT-4o Hurst et al. [2024]. Leveraging multiple proxy reasoners helps mitigate potential bias from any single model when estimating the effectiveness of different visual prompting strategies. Specifically, we construct keyframes with different visual prompting strategies and provide each prompted keyframe sequence, together with the question, to the proxy reasoner. The proxy model is then prompted to produce a concise reasoning trace and a final answer, while explicitly grounding each reasoning step to spatio-temporal evidence in the frames. To enforce structured grounding, we require the reasoning to include object tags (<obj>), bounding box tags (<box>), and timestamp tags (<t>), which jointly specify the referenced object, its spatial location, and the corresponding moment in the video. Details of the proxy reasoner prompt are provided in Figure 9.

Scoring. Based on the proxy reasoner outputs, we aggregate their predictions to obtain an optimal visual prompt pseudo-label for each question. To select the most effective visual prompt for both grounded reasoning and answer prediction, we consider multiple signals, including answer correctness, spatial grounding quality, and object consistency. Specifically, we first parse the predicted bounding boxes, object names, and final answers from the generated reasoning trajectories. Answer quality is evaluated using accuracy for multiple-choice questions and ROUGE for open-ended answers. For spatial grounding, we compute the IoU between the predicted bounding boxes and the annotated boxes provided in the TVQA+ and VideoEspresso datasets. To measure object consistency, we compute an object matching score between predicted and ground-truth object names using a hierarchical similarity metric that considers exact match, substring match, fuzzy similarity, and word-overlap (Jaccard) matching.

Pseudo-label selection. To aggregate results from the three proxy reasoners, we first filter visual prompting candidates where all three proxy reasoners predict the correct answer. Among these candidates, we select the optimal visual prompt by ranking them according to the average of the spatial IoU and object matching scores.

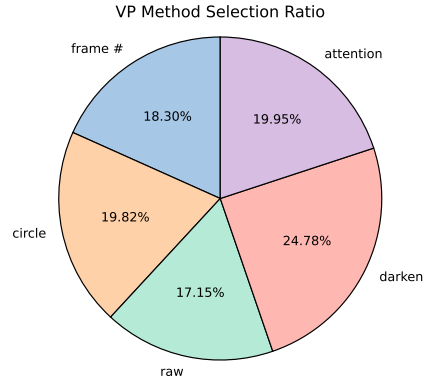


Figure 7: **Distribution selected visual prompting of VP-SELECTOR training datasets.**

C.3 Data Statistics

We use 5,000 training samples from TVQA+ Lei et al. [2020] and 1,382 samples from VideoEspresso Han et al. [2025], both consisting of multiple-choice QA pairs with annotated keyframes and key-object bounding boxes. We additionally include 3,000 samples from the VideoEspresso training set containing open-ended question-answer pairs. The distribution of selected visual prompting methods is illustrated in Figure 7. This distribution indicates that explicit visual prompting is generally beneficial and that the optimal prompting strategy varies across samples.

C.4 Model Architecture

Training. We first formulate visual prompting selection as a generative prediction task without introducing an additional classification head. Each sample consists of the question, optional key object, and video key frames, where multiple frames are combined into a single contact-sheet image. We implement the VP-SELECTOR by fine-tuning Qwen2.5-VL-Instruct (3B) with LoRA Hu et al. [2022], while freezing the backbone parameters. We apply LoRA to the query, key, value, output, and MLP projection layers, with rank $r=16$, scaling $\alpha=32$, and dropout 0.05. We train the model with AdamW for 10 epochs using learning rate 2×10^{-4} , weight decay 0.01, and batch size 8 per process. The model is trained with token-level causal language modeling loss to generate one label from the discrete prompt set $\mathcal{V} = \{\text{api_prompt}, \text{circle}, \text{darken}, \text{numpro}, \text{raw}\}$.

Inference. At inference time, we use greedy decoding and map the generated text to the corresponding prompt class. To obtain the performance reported in Table 6, we first use VP-SELECTOR to predict the optimal visual prompt during inference, apply the selected visual prompting to the original input, and then feed it to each reasoner. If key objects are not provided as annotations (e.g., PerceptionTest), we extract them using Gemini-2.5-Flash Google DeepMind [2025] and apply key-object-based visual prompting. Detailed prompts for key object extraction are provided in Figure 10.

D Additional Analysis

In this section, we present various ablation on V-STAR Cheng et al. [2025b] and VideoMME Fu et al. [2025] using the spatio-temporal category subset of the STGR-RL dataset Meng et al. [2025].

Table 11: Ablation of object-aware spatial reward components on V-STAR and VideoMME.

	Acc	Where (Chain 1)	Where (Chain 2)	mAM	mLGM	VideoMME
Open-o3-video ($r_{\text{spa}}^{\text{max}}$)	58.4	25.4	4.6	30.3	41.4	61.9
+ Average IoU ($r_{\text{spa}}^{\text{avg}}$)	58.7	28.0	5.0	30.1	41.3	61.9
+ Identity matching (r_{spa})	59.9	27.5	5.4	31.3	43.1	62.1

D.1 Ablation of Hyperparameter

In this section, we analyze key hyperparameters of our training framework, including the hard example threshold, the self-distillation loss weight, and the number of self-distillation candidates.

Self-distillation loss weight. As shown in Table 10, we analyze the effect of the self-distillation loss weight α in the overall objective. Introducing self-distillation already provides clear improvements over the baseline without distillation ($\alpha = 0$), improving the answer accuracy from 58.4 to 59.5 even with a small weight ($\alpha = 0.01$). The best performance is achieved at $\alpha = 0.1$, which improves all metrics simultaneously, reaching 60.7 Acc, 31.3 mAM, and 43.1 mLGM. However, further increasing the weight to $\alpha = 0.5$ slightly degrades performance, suggesting that overly strong self-distillation may dominate the RL objective and reduce exploration during training. These results indicate that self-distillation is most effective when used as a moderate auxiliary signal that reinforces high-reward reasoning trajectories without overwhelming the primary GSPO optimization.

Table 10: Ablation of self-distillation loss weight.

α	Acc	mAM	mLGM
0	58.4	30.3	41.4
0.01	59.5	30.4	42.0
0.1 (default)	60.7	31.3	43.1
0.5	60.5	30.9	42.6

D.2 Ablation of Reward

In this section, we analyze the effect of different reward components and spatial reward designs on our training objective.

Ablation of spatial reward design. Prior spatial reward Meng et al. [2025] typically encourages models to localize only a single region by assigning a reward based on the maximum IoU with any ground-truth box. However, grounded video reasoning often requires identifying multiple objects involved in the reasoning process. To better support such behavior, we further ablate the effect of each component in our object-aware spatial grounding reward. Using the same notation as our final reward, we first consider the spatial reward used in prior work Meng et al. [2025], which applies temporal gating but ignores object identity and assigns reward using only the maximum IoU with any ground-truth box:

$$r_{\text{spa}}^{\text{max}}(x, y) = \frac{1}{M} \sum_{m=1}^M \mathbf{1}[\Delta t_m \leq \tau] \max_{b^{\text{gt}} \in \mathcal{B}^{\text{gt}}(\tilde{t}_m)} \text{IoU}(b_m, b^{\text{gt}}). \quad (13)$$

We then replace the max operator with an average over *all* ground-truth boxes at the matched frame, yielding:

$$r_{\text{spa}}^{\text{avg}}(x, y) = \frac{1}{M} \sum_{m=1}^M \mathbf{1}[\Delta t_m \leq \tau] \frac{1}{|\mathcal{O}^{\text{gt}}(\tilde{t}_m)|} \sum_{o \in \mathcal{O}^{\text{gt}}(\tilde{t}_m)} \max_{b^{\text{gt}} \in \mathcal{B}^{\text{gt}}(\tilde{t}_m)} \text{IoU}(b_m, b^{\text{gt}}). \quad (14)$$

Finally, our full object-aware spatial grounding reward further incorporates soft identity matching and averages IoU only over temporally aligned predictions with valid object matches:

$$r_{\text{spa}}(x, y) = \frac{1}{|\mathcal{I}|} \sum_{m \in \mathcal{I}} \frac{1}{|\mathcal{O}_m^{\text{match}}|} \sum_{o \in \mathcal{O}_m^{\text{match}}} \max_{b^{\text{gt}} \in \mathcal{B}^{\text{gt}}(\tilde{t}_m)} \text{IoU}(b_m, b^{\text{gt}}). \quad (15)$$

As shown in Table 11, replacing the max-IoU design with Average IoU improves grounding-related metrics, indicating that aggregating signals from multiple objects provides richer spatial supervision.

Table 13: Ablation of visual prompting assignment to hard samples on V-STAR and VideoMME.

Gating method	Acc	mAM	mLGM	VideoMME
-	59.6	30.4	41.6	61.9
Fixed (darken)	58.3	29.7	40.6	62.4
Fixed (circle)	57.7	29.3	39.9	62.0
Gating (darken, frame#)	59.6	30.6	42.7	62.6
VP-SELECTOR	60.7	31.3	43.1	62.8

Further incorporating identity matching leads to consistent gains across all benchmarks, confirming that enforcing object-level consistency is crucial for grounded reasoning. In contrast, directly averaging IoU across predicted boxes is less effective because many low-quality or irrelevant predictions dilute the supervision signal.

We further analyze how different spatial rewards affect grounding behavior in Table 12. The max-IoU reward from Open-o3-video Meng et al. [2025] results in very few number predicted objects (0.25) and boxes (0.38) in predicted reasoning, reflecting a tendency toward single-region grounding. Introducing Average IoU substantially increases the number of grounded objects (0.70) and boxes (1.18), indicating that multi-object supervision encourages richer spatial reasoning. With identity matching, the model further improves both quantities while maintaining object-level consistency, demonstrating that our reward promotes more faithful multi-object grounding during reasoning.

D.3 Ablation of Visual Prompting Assignment

We evaluate the effectiveness of VP-SELECTOR during RL by replacing it with fixed visual prompting and a simple gating strategy. For the fixed setting, when a hard sample is detected, a predefined visual prompt is applied to the key frame. For the gating, different visual prompts are assigned based on reward signals: if the temporal reward is below the average, we apply frame numbering to the key frame; if the spatial reward is below the average, we apply darkening to the key region. As shown in Table 13, applying a single prompt type to all hard samples (e.g., darken or circle) slightly degrades overall reasoning performance compared to the baseline, suggesting that different questions require different forms of visual guidance. The reward-based gating strategy improves grounding metrics (mAM and mLGM) and slightly boosts VideoMME performance, but its gains remain limited due to the coarse heuristic used for prompt assignment. In contrast, our learned VP-SELECTOR achieves the best performance across all metrics, improving both answer accuracy and grounding quality. These results highlight the importance of adaptive visual prompt selection conditioned on the input video and question for effectively guiding spatio-temporal reasoning during RL training.

Table 12: Average number of predicted objects and bounding boxes per generated reasoning.

	Avg.obj	Avg.box
Open-o3-video (r_{spa}^{max})	0.25	0.38
+ Average IoU (r_{spa}^{avg})	0.70	1.18
+ Identity matching (r_{spa})	0.83	1.40

E Visualization

In Figure 8, we compare grounded reasoning between Open-o3-video and VISIONCOACH. Open-o3-video produces an incorrect answer (“white”) despite providing plausible explanations, indicating potential reliance on language priors rather than visual evidence. In contrast, VISIONCOACH correctly identifies the nail color (“pink”) and supports the answer with precise spatial grounding on the woman’s hands across frames. This example illustrates that VISIONCOACH encourages reasoning grounded with more reliable visual evidence, leading to more accurate predictions.

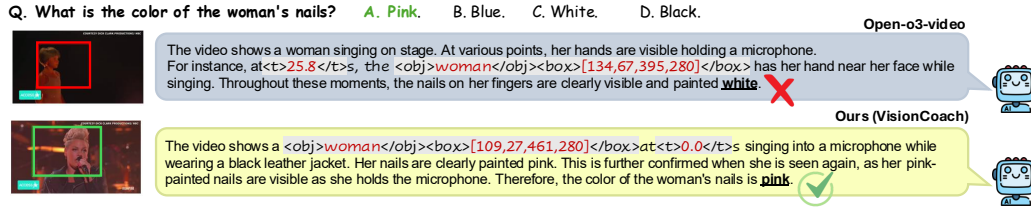


Figure 8: Comparison of grounding with Open-o3-video and VISIONCOACH.

F Limitation and Future Work

While VISIONCOACH demonstrates strong improvements in grounded video reasoning, several limitations remain. First, the framework still relies on training signals derived from grounding annotations (e.g., object boxes and temporal locations) to construct the spatial and temporal rewards. Although such annotations are available in many research benchmarks, scaling this approach to domains where precise grounding supervision is scarce may require additional strategies for obtaining reliable reward signals. Second, the effectiveness of VisionCoach depends on the quality of the visual prompts selected during training. Although the VP-Selector learns to choose prompts adaptively, the prompt candidate pool is predefined and relatively simple (e.g., circles, darkening, frame indicators). More expressive forms of visual guidance or learned prompt generation may further improve the training signal for complex reasoning scenarios. Future work may explore more efficient training strategies or scalable RL formulations to further improve practicality when applying the framework to larger video models and datasets.

Prompt to the proxy reasoner

You are a spatio-temporal video question answering model.

You will be given:

- A multiple-choice question with 5 options (A, B, C, D, E).
- K keyframes from a video in chronological order.

Some frames may contain visual prompts (e.g., boxes/circles/darkening/heatmaps or frame-number overlays).

Use these visual prompts as grounding hints when helpful.

Your job:

- 1) Produce a short, evidence-grounded reasoning that explicitly cites objects, bounding boxes, and timestamps using special tags.
- 2) Select the correct answer (A, B, C, D, or E).

OUTPUT FORMAT (MUST FOLLOW EXACTLY):

Return ONLY a valid JSON dictionary with exactly two keys: "reasoning" and "answer".

- "reasoning": a single paragraph string that includes grounding tags.
- "answer": a single string with the final answer (must be one of: "A", "B", "C", "D", or "E").

GROUNDING TAG REQUIREMENTS (MANDATORY):

- Object tag: `<obj>...</obj>`
- Box tag: `<box>[x1, y1, x2, y2]</box>`
- Time tag: `<t>...</t>` (seconds)

Each grounding claim in the reasoning MUST include `<obj>`, `<box>`, and `<t>` together. Use the exact substring pattern: `<obj>OBJECT</obj><box>[x1, y1, x2, y2]</box>at<t>TIME</t>s`

Return format:

```
{ "reasoning": "...<obj>...</obj><box>...</box>at<t>...</t>s...", "answer": "A" }
```

Rules:

- The reasoning must not exceed 200 words.
- Use integer box coordinates in [0, 999].
- The answer must be exactly one letter: A, B, C, D, or E.

Figure 9: Prompt to proxy reasoner.

Key object selection prompt by Gemini-2.5-Flash

You are given a question, list of candidate visual objects and its answer about a video.

Your task is to identify the key visual object(s) that must be visually grounded to make the answer correct. Select ONE primary visual object, and optionally up to TWO secondary visual objects.

[Question]
{question}

[Extracted objects]
{objects}

[Answer]
{answer}

Selection rules:

- Prefer selecting object names from [Extracted objects] if they reasonably match the question and answer.
- Only select a new object NOT in [Extracted objects] if none of the extracted objects are reasonable.
- If there is NO specific object that needs to be grounded (e.g., abstract, scene-level, or judgment-based questions), return "NONE" as the primary object.
- For "used_object", indicate whether each object (primary and secondary) comes from [Extracted objects]:
 - "yes" if the object is in [Extracted objects]
 - "no" if the object is newly selected (not in [Extracted objects]) or if primary is "NONE"

Output JSON only in the following format:

```
{  
  "primary": "object name or NONE",  
  "secondary": ["object name", ...],  
  "used_object": {  
    "primary": "yes" or "no",  
    "secondary": ["yes" or "no", ...] // same length as secondary array  
  }  
}
```

Figure 10: Prompt for extracting key object from question and answer pair.